

A sticky bacterium versus antiadhesive surfaces: The adhesion preference of bacteria expressing trimeric autotransporter adhesin

Short title: A sticky bacterium versus antiadhesive surfaces

S. Yoshimoto¹, A. Kawashiri¹, T. Matsushita², S. Ishii¹, S. Göttig³, V. A. J. Kempf³, M. Takai², K. Hori^{1*}

¹Department of Biomolecular Engineering, Graduate School of Engineering, Nagoya University, Nagoya, Aichi 464-8603, Japan.

²Department of Bioengineering, Graduate School of Engineering, The University of Tokyo, Bunkyo-ku, Tokyo 133-8656, Japan.

³Institute for Medical Microbiology and Infection Control, University Hospital, Goethe University, Frankfurt 60596, Germany.

*Correspondence to: khori@chembio.nagoya-u.ac.jp

Abstract

While microorganisms have evolved to adhere and form biofilms on surfaces, various materials with antiadhesive surfaces have been developed. The Gram-negative bacterium *Acinetobacter* sp. Tol 5 exhibits high adhesiveness to various surfaces through AtaA, one of trimeric autotransporter adhesins (TAAs). We examined the adhesion of Tol 5 and other bacteria expressing different TAAs to antiadhesive surfaces. The results highlighted Tol 5's stickiness through AtaA, which enables cells to adhere even to antiadhesive materials including polytetrafluoroethylene with a low surface free energy, a hydrophilic polymer brush exerting steric hindrance, and mica with an ultrasmooth surface. Tol 5 cells also adhered to a zwitterionic 2-methacryloyloxyethyl-phosphorylcholine-polymer-coated surface but were exfoliated by a weak shear stress, suggesting that exchangeable bound water molecules contribute to AtaA's interaction with materials.

31 Introduction

32 Pathogenic bacteria, like viruses, cause infectious diseases, and the threat is reminded by the
33 COVID-19 pandemic. However, bacteria are not as much of a threat as viruses because antibiotics
34 are effective against them. This is changing, however, with the emergence of antibiotic-resistant
35 bacteria. The global expansion of multidrug-resistant bacteria has become a clinical problem (1),
36 and the threat of bacterial infection might come back in the near future. The overuse of antibiotics
37 amplifies the opportunity for resistant bacteria to emerge and spread (2). The increased antibiotic
38 use during this COVID-19 pandemic could also increase the threat of resistant bacteria (3). As an
39 alternative to antibiotics, antiadhesive (antibiofouling) surfaces have drawn intensive research
40 interest because bacterial adhesion is the initial step of infection by pathogens and biofouling of
41 equipment (4-7). As a result of extensive efforts, various antiadhesive surfaces have been
42 developed and characterized, such as fluoropolymers, polymer brushes, highly hydrophilic
43 zwitterionic polymers, and ultrasmooth or nano/micro-topographical patterned surfaces (8-12).

44 *Acinetobacter* sp. Tol 5, which is a toluene-degrading bacterium that we previously isolated from
45 a biofiltration system, exhibits autoagglutination and high adhesiveness to solid surfaces (13, 14).
46 Tol 5 cells quickly adhere to various material surfaces from hydrophobic plastics to hydrophilic
47 glasses and metals independently of biofilm formation (13). This characteristic nonspecific
48 adhesiveness of Tol 5 cells is mediated by AtaA, a member of the trimeric autotransporter adhesin
49 (TAA) family (15-17). TAAs are outer membrane proteins of Gram-negative bacteria and have
50 been well-studied as virulence factors because each TAA shows an ability to bind to biotic
51 molecules of mammalian host cells and occasionally to some kinds of abiotic surfaces (18, 19).
52 Although they have a variety of lengths from several hundreds to several thousands of amino
53 acids, they have a common structure that includes an N-terminal passenger domain (PSD), which
54 is secreted onto the cell surface and is responsible for its function, and a C-terminal
55 transmembrane domain, which anchors the PSD onto the outer membrane (19). AtaA is one of the
56 largest TAAs consisting of 3,630 amino acids but shares common structural features with other
57 TAAs, (15, 20). However, there have been no reports of TAA-mediated adhesion similar to Tol 5
58 cells through AtaA in terms of nonspecificity and high stickiness.

59 In a proverb known as the “shield-spear contradiction” derived from an ancient Chinese text *Han*
60 *Feizi*, a merchant first boasts that, “this shield is strong enough to prevent anything,” and then,
61 “this spear is sharp enough to pierce anything.” In response to the merchant’s boasting, one
62 person from the crowd asks the merchant, “What would happen if you attack your shield with
63 your spear?” The merchant could not answer. Similarly, we also don’t know what would happen
64 if highly adhesive Tol 5 cells encounter an antiadhesive surface. In this study, we investigated the
65 interaction of Tol 5 and some other TAA-expressing bacterial cells with various surfaces
66 including antiadhesive surfaces that have different repelling mechanisms.

67 Results

68 Outstanding adhesiveness mediated by AtaA compared with other TAAs

69 First, we compared the adhesiveness of Tol 5 and its $\Delta ataA$ mutant (negative control) with that of
70 *Yersinia enterocolitica* and *Bartonella henselae* by shaking each cell suspension in the presence
71 of a polyurethane support for 30 min. These Gram-negative bacteria have also been reported to
72 adhere to abiotic surfaces through their TAAs (18), YadA and BadA, respectively. The
73 production of these TAAs was confirmed by western blotting (see Supplementary Figure S1). The
74 result showed the overwhelming stickiness of cells expressing AtaA compared with that of cells
75 expressing the other TAAs (Fig. 1). Most of the Tol 5 cells adhered to the support and the cell
76 suspension became abundantly clear. In contrast, the cell suspensions of *Y. enterocolitica*, *B.*
77

78 *henselae*, and Tol 5 Δ *ataA* mutant remained cloudy, which indicated that many of the cells did not
79 adhere to the polyurethane support.

80 Next, we quantified the adhesiveness of bacterial cells that express TAAs to various material
81 surfaces. Cell suspensions were placed and incubated on polystyrene (PS), glass, stainless steel,
82 and polytetrafluoroethylene (PTFE, known as Teflon) surfaces for 10 min. Non-adhering cells
83 were removed by washing with a fresh medium and the adhered cells on the material surface were
84 quantified by crystal violet staining. As shown in Figure 2, in a short time (10 min), Tol 5 could
85 adhere to not only PS, glass, and stainless steel but also to PTFE, which has antiadhesive
86 properties derived from its low surface energy (8). In contrast, Tol 5 Δ *ataA* mutant and *Y.*
87 *enterocolitica* hardly adhered to all the material surfaces. Although *B. henselae* showed
88 measurable adhesiveness, the amount of adhered cells was much smaller than that of Tol 5. These
89 results quantitatively demonstrated that Tol 5 cells exhibit remarkably higher adhesiveness to
90 various material surfaces through AtaA than bacterial cells expressing other TAAs.

91 **AtaA versus antiadhesive surfaces**

92 To investigate whether Tol 5 cells adhere to various other antiadhesive surfaces in addition to
93 PTFE, we performed adhesion assays with mica, poly(oligo(ethylene glycol) methyl ether
94 methacrylate) (poly(mOEGMA)) brush, and 2-methacryloyloxyethyl phosphorylcholine (MPC)
95 polymer surfaces. Mica is a phyllosilicate mineral of aluminum and potassium, and its surface
96 after cleaving is atomically flat (21). A poly(mOEGMA) brush is a neutral hydrophilic polymer
97 brush and exerts steric repulsion (10). An MPC polymer is a zwitterionic hydrophilic polymer and
98 possesses a high free water fraction (22). These surfaces have been reported to have antiadhesive
99 properties against bacterial cells (9, 11, 23). After incubation of bacterial cells on the antiadhesive
100 surfaces for 10 min, Tol 5 cells adhered to PTFE but not to the mica, poly(mOEGMA) brush, and
101 MPC polymer surface (Fig. 3A). After incubation for 2 h, Tol 5 cells adhered to not only PTFE
102 but also to the mica and poly(mOEGMA) brush surface, but hardly adhered to the MPC polymer
103 (Fig. 3A). In contrast, *B. henselae* adhered to PTFE and mica but not to the poly(mOEGMA)
104 brush and the MPC polymer (Fig. 3B). These results emphasize that Tol 5 cells were the only
105 cells that adhered to the poly(mOEGMA) brush and showed that even sticky Tol 5 cells hardly
106 adhered to the MPC polymer under these experimental conditions.

107 **Cell behavior caused by AtaA on a MPC polymer surface**

108 To investigate how the MPC polymer repels Tol 5 cells, we observed the behavior of Tol 5 cells
109 on the polymer surface by using a flow cell system with a square glass tube (Fig. 4A) (24). The
110 glass tube with or without the MPC polymer coating was filled with a Tol 5 cell suspension and
111 incubated for 10 min. Then, the cell suspension was replaced with fresh BS-N medium by slow
112 flowing at 10 μ L/min for rinsing, and the flow rate was increased stepwise, as shown in Figure 4B,
113 while observing the inner surface of the bottom of the glass tube under a microscope.
114 Unexpectedly, Tol 5 cells adhered to the MPC-polymer-coated glass as much as the bare (non-
115 coated) glass under static conditions and remained adhered after rinsing at 10 μ L/min (Fig 4C
116 initial). When the flow rate was increased to 20 μ L/min, a small fraction of previously adhered
117 cell clumps started to move and slip on the surface (see Supplementary Movie S1), but many cells
118 still resisted detachment after 10 min of flowing (Fig. 4C, 20 μ L/min). At a high flow rate of 50
119 μ L/min or more, the Tol 5 cells firmly adhered to the bare glass whereas the cells attached on the
120 MPC polymer were exfoliated, rolled, and washed off from the surface by the shear stress (≥ 5.94
121 mN/m²) (Fig. 4C, ≥ 50 μ L/min and see Supplementary Movie S1).

122
123
124 **Discussion**

125 So far, various antiadhesive materials have been developed on the basis of repelling mechanisms.
126 Fluoropolymers with a low surface free energy are widely used in cookware and medical

equipment although their hydrophobicity is also said to cause protein adsorption that hinders cell attachment by contraries (25). Polymer brushes with a high grafting density have been especially studied as powerful antiadhesive surfaces for cell adhesion (26). However, the finding that *Acinetobacter* sp. Tol 5 is able to adhere to these antiadhesive materials makes us realize the marvel of microbial diversity and evolution. In addition, AtaA could mediate cell adhesion to poly(mOEGMA) brush but BadA could not. Note that BadA is similar to AtaA in size and abundance on the cell surface; it consists of 3,082 amino acids and its fibrous molecules peritrichately cover over bacterial cells (18). Therefore, their difference in adhesiveness demonstrates the functional diversity of the TAA family as a result of protein evolution.

Tol 5 cells even adhered to an MPC-polymer-coated surface but their interaction was so weak that the cells could be exfoliated by a weak shear stress. The exfoliated and rolling cell clumps seemed to involve and remove cell clumps that were still adhered owing to the autoagglutinating property of Tol 5 cells (24), self-cleaning the surface coated with the MPC polymer. In an adhesion assay using a microwell, the Tol 5 cells should have been detached by the washing step. MPC is a methacrylate monomer with a phosphorylcholine (PC) group, which is a hydrophilic polar head group of phospholipids comprising a eukaryotic cell membrane (27). MPC polymers are known to significantly suppress adhesion of proteins and cells because there are lots of free water molecules (22) but capture few bound water molecules on their PC group (27-29). The fact that Tol 5 cells can adhere to the poly(mOEGMA) brush and the mica, but can only interact very weakly with a surface coated with MPC polymers, despite similar levels of hydrophilicity, as shown by the static contact angles of air in water (Table S2), suggests that exchangeable bound water molecules contribute to the interaction between AtaA and material surfaces (28).

Materials and Methods

Materials

The polyurethane foam support (1 cm³ cube; CFH-30) was obtained from Inoac Corporation (Aichi, Japan). The polystyrene plate (PS2035-1), glass plate (FF-001), stainless steel plate (SUS430 grade; EA441WA-21), PTFE plate (J1-537-01), mica disk (V-1 grade), and square glass tube (VitroTubes, 8100) were purchased from Hikari Co., Ltd. (Osaka, Japan), Matsunami Glass Ind., Ltd. (Osaka, Japan), ESCO Co., Ltd. (Osaka, Japan), AS ONE Corp. (Osaka, Japan), TED PELLA, Inc. (CA, USA), and Vitrocom (Mountain Lakes, NJ), respectively. The poly(mOEGMA) brush surface was prepared as described previously (29). Prior to use, glass was washed with piranha solution followed by rinsing with pure water, mica was cleaved with scotch tape, and stainless steel and PTFE were rinsed with pure ethanol.

The MPC-polymer-coated surface for the adhesion assays was prepared as described below. A glass plate was dipped into 2% MPC polymer (Lipidure-CM5206, a copolymer of MPC and butyl methacrylate; NOF Corp., Tokyo, Japan) solution dissolved in ethanol and shaken at 70 rpm for 3 min. After shaking, the glass plate was rinsed in pure water and dried at 60°C for 3 h.

The MPC-polymer-coated glass tube was prepared as described below using the flow cell system. A solution of 2% MPC polymer dissolved in ethanol was flowed through the square glass tube (50 mm in length and 1 mm in every internal dimension) at 100 μ L/min for 3 min, and then pure water was flowed through at 500 μ L/min for 2 min. After passing air through at 500 μ L/min for 2 min, the glass tube was removed from the flow cell system and dried at 60°C for 3 h.

The static contact angles of air bubbles (SCA) in water on each material surface were measured with a contact angle meter (CA-W, Kyowa Interface Science Co., Tokyo, Japan) at room temperature and listed in Supplementary Table S2. Material substrates were immersed in water, and 10 μ L of air bubbles were placed on the substrates.

Microwells used in the adhesion assays to various material surfaces were self-made as follows: Four sheets of vinyl electrical tape (ASKUL Corporation, Tokyo, Japan) were piled up and holes

with a diameter of 6 mm were punched. The punched tapes were placed on a material plate as shown in Supplementary Figure S2.

Bacterial strains and culture conditions

The bacterial strains used in this study are listed in Supplementary Table S1. These bacterial strains were grown as previously described (15, 30). *Acinetobacter* strains were grown in Luria-Bertani (LB) medium at 28°C for 8 h. An overnight culture of *Yersinia enterocolitica* strains grown in LB medium at 28°C was used to inoculate LB medium at a 1:100 dilution, and the medium was incubated at 37°C for 6 h. *Bartonella henselae* strains were grown for 5 days on Columbia agar supplemented with 5% sheep blood at 37°C in a humidified atmosphere with 5% CO₂. Expression of trimeric autotransporter adhesins in each strain was confirmed by western blotting using anti-AtaA₆₉₉₋₁₀₁₄ antiserum, anti-BadA antibody (31), and anti-YadA antibody (sc-22472; Santa Cruz Biotechnology, Inc., Dallas, TX, USA).

Adhesion assays to polyurethane foam support

The adhesion assays to polyurethane foam support were performed as previously described (32), with slight modifications. Bacterial cells were suspended in BS-N medium (33) (containing no carbon or nitrogen sources), and the optical density of the cell suspension at 660 nm (OD₆₆₀) was adjusted to 1.0. Four pieces of the polyurethane foam support were placed into 20 mL of the cell suspension and shaken at 115 rpm at 28°C. After a 30-min incubation with shaking, the transparency of the cell suspension was observed and photographed by a digital camera.

Microwell adhesion assay

Bacterial cells were suspended in BS-N medium and the OD₆₆₀ was adjusted to 0.5. The cell suspensions (50 µL each) were placed into the microwell on the materials and incubated at 28°C for 10 min. When the antiadhesive surfaces were used, the incubation time was extended to 30 min and 2 h. The cell suspensions were removed using a pipet after the incubation and the wells were washed for 10 s by shaking in BS-N medium at 70 rpm. Cells adhering in the well were stained with 50 µL of 0.1% crystal violet solution for 15 min and washed for 10 s by shaking in BS-N medium at 70 rpm. Finally, the stain was eluted with 200 µL of 70% ethanol, and the absorbance of the elution at 590 nm (A₅₉₀) was measured with a microplate reader (ARVO X3; PerkinElmer, Inc., MA, USA).

Flow cell system

The rectangular flow cell system, which we have previously reported (24), was used with slight modifications: a syringe pump (Legato 200; KD Scientific, Holliston, MA) was directly connected to the square glass tube without using a three-way stopcock valve. Tol 5 cells were suspended in BS-N medium at an OD₆₆₀ of 0.2, and the suspension was subjected to sonication to break up the cell clumps. The glass tube with or without an MPC polymer coating was filled with the cell suspension and incubated for 10 min at room temperature. The suspension was replaced with fresh BS-N medium by slow flowing at 10 µL/min for 35 min and the flow rate was increased stepwise. Live images of the behavior of Tol 5 cells during their adhesion and detachment to/from the inner surface of the glass tube were recorded under a digital microscope (VHX-200; Keyence, Osaka, Japan). Wall shear stress was calculated as previously described (24).

H2: Supplementary Materials

Fig. S1. Production of trimeric autotransporter adhesin (TAA) in each bacterial cell.

Fig. S2. Preparation of microwells on material surfaces.

Table S1. Bacterial strains used in this study.

Table S2. Static contact angles (SCA) of air in water of material surfaces.

Movie S1. Detachment of adhered Tol 5 cells from the MPC polymer coated glass.

References and Notes

1. S. Baker, N. Thomson, F. X. Weill, K. E. Holt, Genomic insights into the emergence and spread of antimicrobial-resistant bacterial pathogens. *Science* **360**, 733-738 (2018).
2. "WHO report on surveillance of antibiotic consumption: 2016-2018 early implementation," World Health Organization (2018).
3. J. Hsu, How covid-19 is accelerating the threat of antimicrobial resistance. *BMJ* **369**, m1983 (2020).
4. I. Banerjee, R. C. Pangule, R. S. Kane, Antifouling coatings: Recent developments in the design of surfaces that prevent fouling by proteins, bacteria, and marine organisms. *Adv Mater* **23**, 690-718 (2011).
5. C. Berne, C. K. Ellison, A. Ducret, Y. V. Brun, Bacterial adhesion at the single-cell level. *Nat Rev Microbiol* **16**, 616-627 (2018).
6. L. Hall-Stoodley, J. W. Costerton, P. Stoodley, Bacterial biofilms: From the natural environment to infectious diseases. *Nat Rev Microbiol* **2**, 95-108 (2004).
7. K. Hori, S. Matsumoto, Bacterial adhesion: From mechanism to control. *Biochem Eng J* **48**, 424-434 (2010).
8. C. I. Pereni, Q. Zhao, Y. Liu, E. Abel, Surface free energy effect on bacterial retention. *Colloid Surface B* **48**, 143-147 (2006).
9. G. Cheng, Z. Zhang, S. F. Chen, J. D. Bryers, S. Y. Jiang, Inhibition of bacterial adhesion and biofilm formation on zwitterionic surfaces. *Biomaterials* **28**, 4192-4199 (2007).
10. M. C. Sin, S. H. Chen, Y. Chang, Hemocompatibility of zwitterionic interfaces and membranes. *Polym J* **46**, 436-443 (2014).
11. G. H. Zeng, T. Muller, R. L. Meyer, Single-cell force spectroscopy of bacteria enabled by naturally derived proteins. *Langmuir* **30**, 4019-4025 (2014).
12. J. Hasan, K. Chatterjee, Recent advances in engineering topography mediated antibacterial surfaces. *Nanoscale* **7**, 15568-15575 (2015).
13. M. Ishikawa, K. Shigemori, A. Suzuki, K. Hori, Evaluation of adhesiveness of *Acinetobacter* sp. Tol 5 to abiotic surfaces. *J Biosci Bioeng* **113**, 719-725 (2012).
14. K. Hori, S. Yamashita, S. Ishii, M. Kitagawa, Y. Tanji, H. Unno, Isolation, characterization and application to off-gas treatment of toluene-degrading bacteria. *J Chem Eng Jpn* **34**, 1120-1126 (2001).
15. M. Ishikawa, H. Nakatani, K. Hori, AtaA, a new member of the trimeric autotransporter adhesins from *Acinetobacter* sp. Tol 5 mediating high adhesiveness to various abiotic surfaces. *PLoS One* **7**, e48830 (2012).
16. K. Noba, M. Ishikawa, A. Uyeda, T. Watanabe, T. Hohsaka, S. Yoshimoto, T. Matsuura, K. Hori, Bottom-up creation of an artificial cell covered with the adhesive bacterionanofiber protein AtaA. *J Am Chem Soc* **141**, 19058-19066 (2019).
17. S. Yoshimoto, H. Nakatani, K. Iwasaki, K. Hori, An *Acinetobacter* trimeric autotransporter adhesin reaped from cells exhibits its nonspecific stickiness via a highly stable 3D structure. *Sci Rep* **6**, 28020 (2016).
18. N. F. Muller, P. O. Kaiser, D. Linke, H. Schwarz, T. Riess, A. Schafer, J. A. Eble, V. A. J. Kempf, Trimeric autotransporter adhesin-dependent adherence of *Bartonella henselae*, *Bartonella quintana*, and *Yersinia enterocolitica* to matrix components and endothelial cells under static and dynamic flow conditions. *Infect Immun* **79**, 2544-2553 (2011).
19. D. Linke, T. Riess, I. B. Autenrieth, A. Lupas, V. A. J. Kempf, Trimeric autotransporter adhesins: variable structure, common function. *Trends Microbiol* **14**, 264-270 (2006).

20. K. Koiwai, M. D. Hartmann, D. Linke, A. N. Lupas, K. Hori, Structural basis for toughness and flexibility in the C-terminal passenger domain of an *Acinetobacter* trimeric autotransporter adhesin. *J Biol Chem* **291**, 3705-3724 (2016).
21. W. de Poel, S. Pintea, J. Drnec, F. Carla, R. Felici, P. Mulder, J. A. A. W. Elemans, W. J. P. van Enkevort, A. E. Rowan, E. Vlieg, Muscovite mica: Flatter than a pancake. *Surf Sci* **619**, 19-24 (2014).
22. K. Ishihara, H. Nomura, T. Mihara, K. Kurita, Y. Iwasaki, N. Nakabayashi, Why do phospholipid polymers reduce protein adsorption? *J Biomed Mater Res* **39**, 323-330 (1998).
23. T. Kameda, K. Ohkuma, S. Oka, Polytetrafluoroethylene (PTFE): A resin material for possible use in dental prostheses and devices. *Dent Mater J* **38**, 136-142 (2019).
24. Y. Furuichi, K. Iwasaki, K. Hori, Cell behavior of the highly sticky bacterium *Acinetobacter* sp. Tol 5 during adhesion in laminar flows. *Sci Rep* **8**, 8285 (2018).
25. Z. K. Zander, M. L. Becker, Antimicrobial and antifouling strategies for polymeric medical devices. *ACS Macro Lett* **7**, 16-25 (2018).
26. M. Krishnamoorthy, S. Hakobyan, M. Ramstedt, J. E. Gautrot, Surface-initiated polymer brushes in the biomedical field: Applications in membrane science, biosensing, cell culture, regenerative medicine and antibacterial coatings. *Chem Rev* **114**, 10976-11026 (2014).
27. Y. Iwasaki, K. Ishihara, Cell membrane-inspired phospholipid polymers for developing medical devices with excellent biointerfaces. *Sci Technol Adv Mat* **13**, 064101 (2012).
28. D. Nagasawa, T. Azuma, H. Noguchi, K. Uosaki, M. Takai, Role of interfacial water in protein adsorption onto polymer brushes as studied by SFG spectroscopy and QCM. *J Phys Chem C* **119**, 17193-17201 (2015).
29. T. Azuma, R. Ohmori, Y. Teramura, T. Ishizaki, M. Takai, Nano-structural comparison of 2-methacryloyloxyethyl phosphorylcholine- and ethylene glycol-based surface modification for preventing protein and cell adhesion. *Colloid Surface B* **159**, 655-661 (2017).
30. Y. Y. Lu, B. Franz, M. C. Truttmann, T. Riess, J. Gay-Fraret, M. Faustmann, V. A. J. Kempf, C. Dehio, *Bartonella henselae* trimeric autotransporter adhesin BadA expression interferes with effector translocation by the VirB/D4 type IV secretion system. *Cell Microbiol* **15**, 759-778 (2013).
31. T. Riess, S. G. E. Andersson, A. Lupas, M. Schaller, A. Schafer, P. Kyme, J. Martin, J. H. Walzlein, U. Ehehalt, H. Lindroos, M. Schirle, A. Nordheim, I. B. Autenrieth, V. A. J. Kempf, *Bartonella* adhesin A mediates a proangiogenic host cell response. *J Exp Med* **200**, 1267-1278 (2004).
32. K. Hori, Y. Ohara, M. Ishikawa, H. Nakatani, Effectiveness of direct immobilization of bacterial cells onto material surfaces using the bacterionanofiber protein AtaA. *Appl Microbiol Biotechnol* **99**, 5025-5032 (2015).
33. H. Watanabe, Y. Tanji, H. Unno, K. Hori, Rapid conversion of toluene by an *Acinetobacter* sp. Tol 5 mutant showing monolayer adsorption to water-oil interface. *J Biosci Bioeng* **106**, 226-230 (2008).
34. M. Ishikawa, K. Hori, A new simple method for introducing an unmarked mutation into a large gene of non-competent Gram-negative bacteria by FLP/FRT recombination. *BMC Microbiol* **13**, 86 (2013).
35. M. Drancourt, R. Birtles, G. Chaumentin, F. Vandenesch, J. Etienne, D. Raoult, New serotype of *Bartonella henselae* in endocarditis and cat-scratch disease. *Lancet* **347**, 441-443 (1996).
36. J. Heesemann, R. Laufs, Construction of a mobilizable *Yersinia enterocolitica* virulence plasmid. *J Bacteriol* **155**, 761-767 (1983).

326
327
328 **Acknowledgments:**

329 **General:** We thank Kai Iio and Eriko Matsui for the adhesion assay. **Funding:** This work was
330 supported by the Japan Society for the Promotion of Science (JSPS) KAKENHI (Grant Numbers
331 JP17H01345, JP18K14062) and by the Deutsche Forschungsgemeinschaft (DFG research group
332 2251). **Author contributions:** K.H. designed the study, and S.Y., A.K., and K.H. wrote the paper.
333 S.Y. and A.K. conducted the adhesion assay. A.K., T.M., and M.D. prepared the poly(mOEGMA)
334 brush surface and measured the static contact angles of air bubbles in water. S.I. and A.K.
335 conducted cultivation and protein analysis of bacterial cells with help from S.G. and V.A.J.K. All
336 authors reviewed the manuscript. **Competing interests:** Authors declare no competing interests.
337 **Data and materials availability:** All data are available in the main text or the supplementary
338 materials.
339
340

341
342
343
344
345
346

Figures and Tables

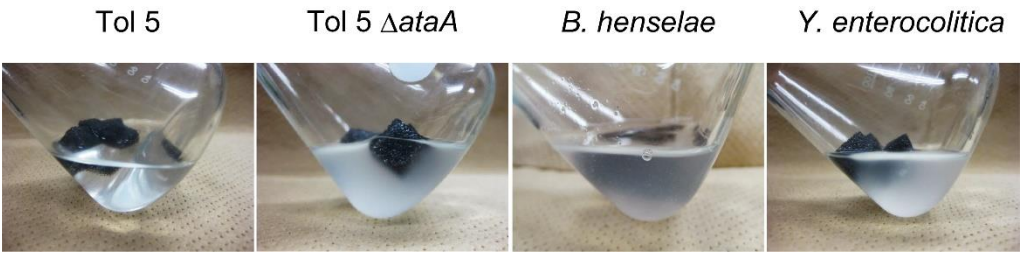


Fig. 1. Adhesion of bacterial cells to a polyurethane surface. Each panel shows the bacterial cell suspension after shaking for 30 min with a polyurethane foam support.

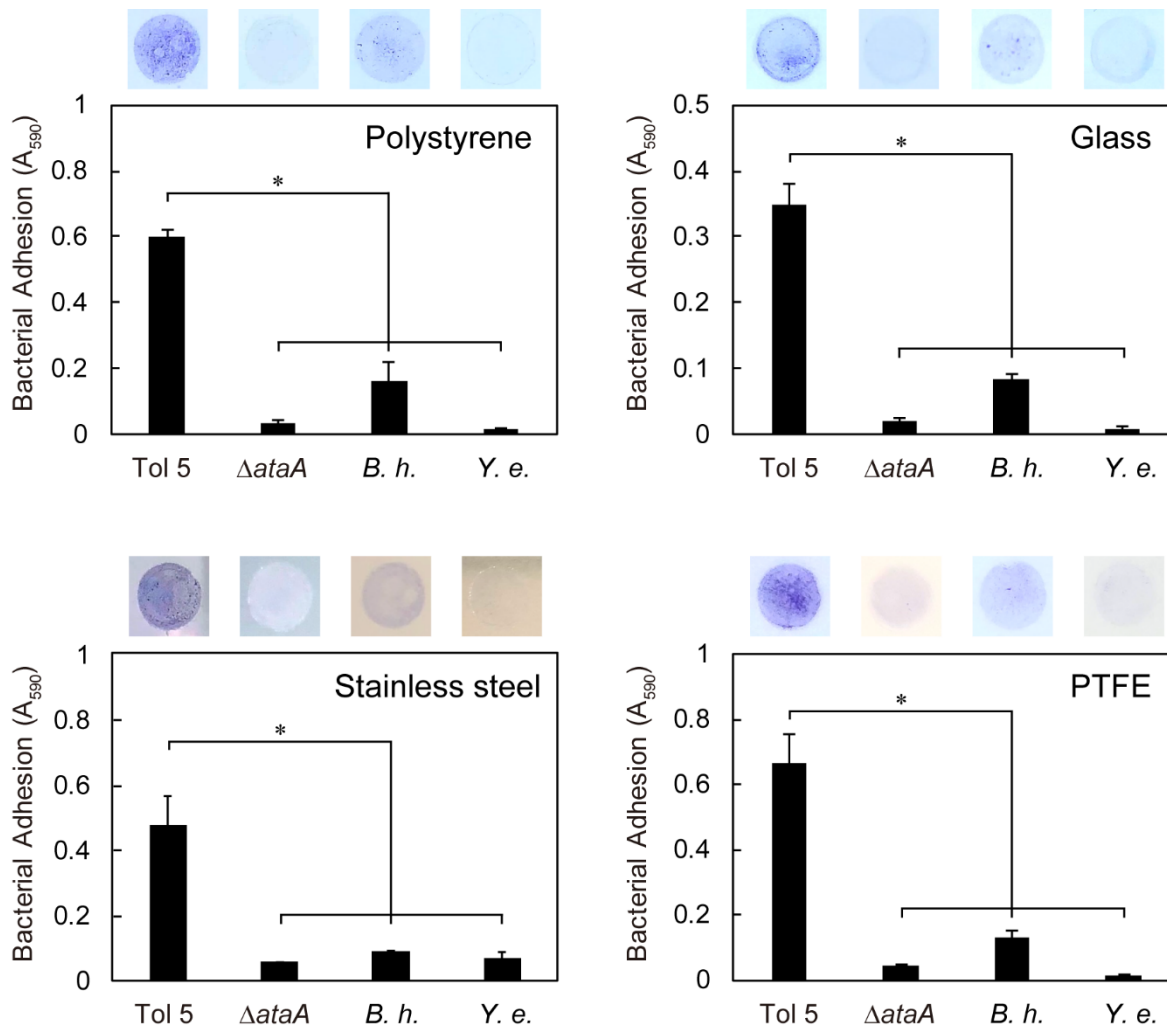
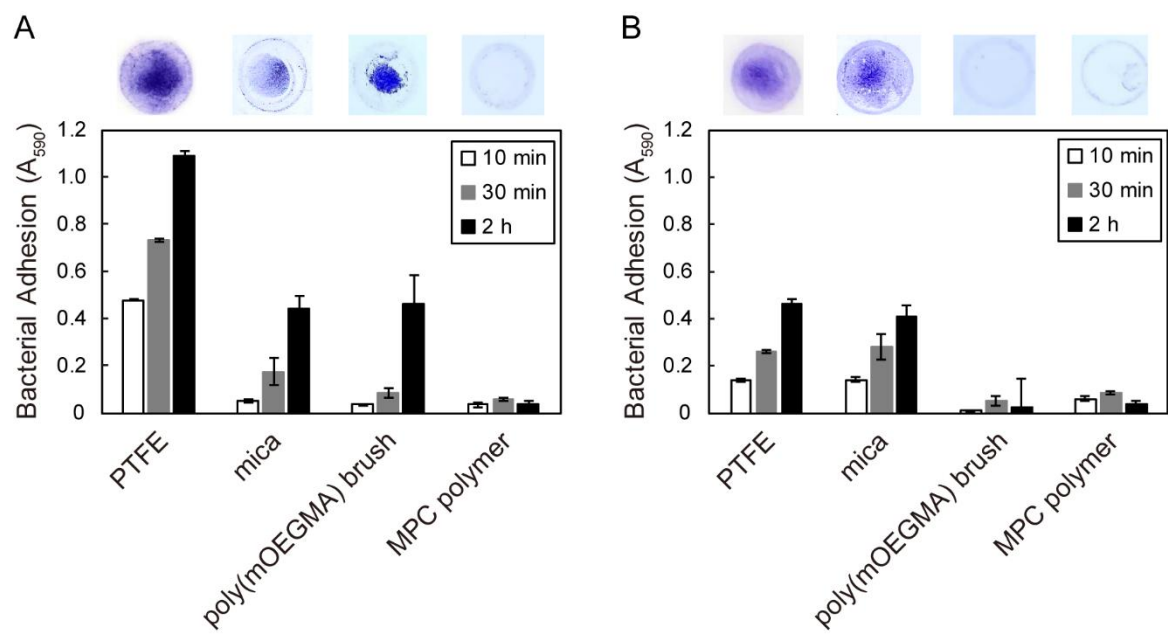


Fig. 2. Adhesion of bacterial cells to various materials. Adhesion of *Acinetobacter* sp. Tol 5, Tol 5 Δ ataA, *B. henselae* (*B. h.*), and *Y. enterocolitica* (*Y. e.*) to polystyrene, glass, stainless steel, and PTFE was assessed by microwell adhesion assays for 10 min. Data are expressed as the mean \pm SEM (n=3). Significant differences from the result of Tol 5, analyzed using Student's t-test, are indicated by an asterisk (p<0.05). Upper photographs show the adhered cells on the material surfaces.

355



356

357 **Fig. 3.** Adhesion of bacterial cells to antiadhesive surfaces. Adhesion of Tol 5 (A) and *B.*
358 *henselae* (B) to PTFE, mica, poly(mOEGMA) brush on glass, and MPC-polymer-coated glass,
359 was assessed by microwell adhesion assays. Data are expressed as the mean \pm SEM (n=3). Upper
360 photographs show the adhered cells on the material surfaces after incubation for 2 h.
361
362

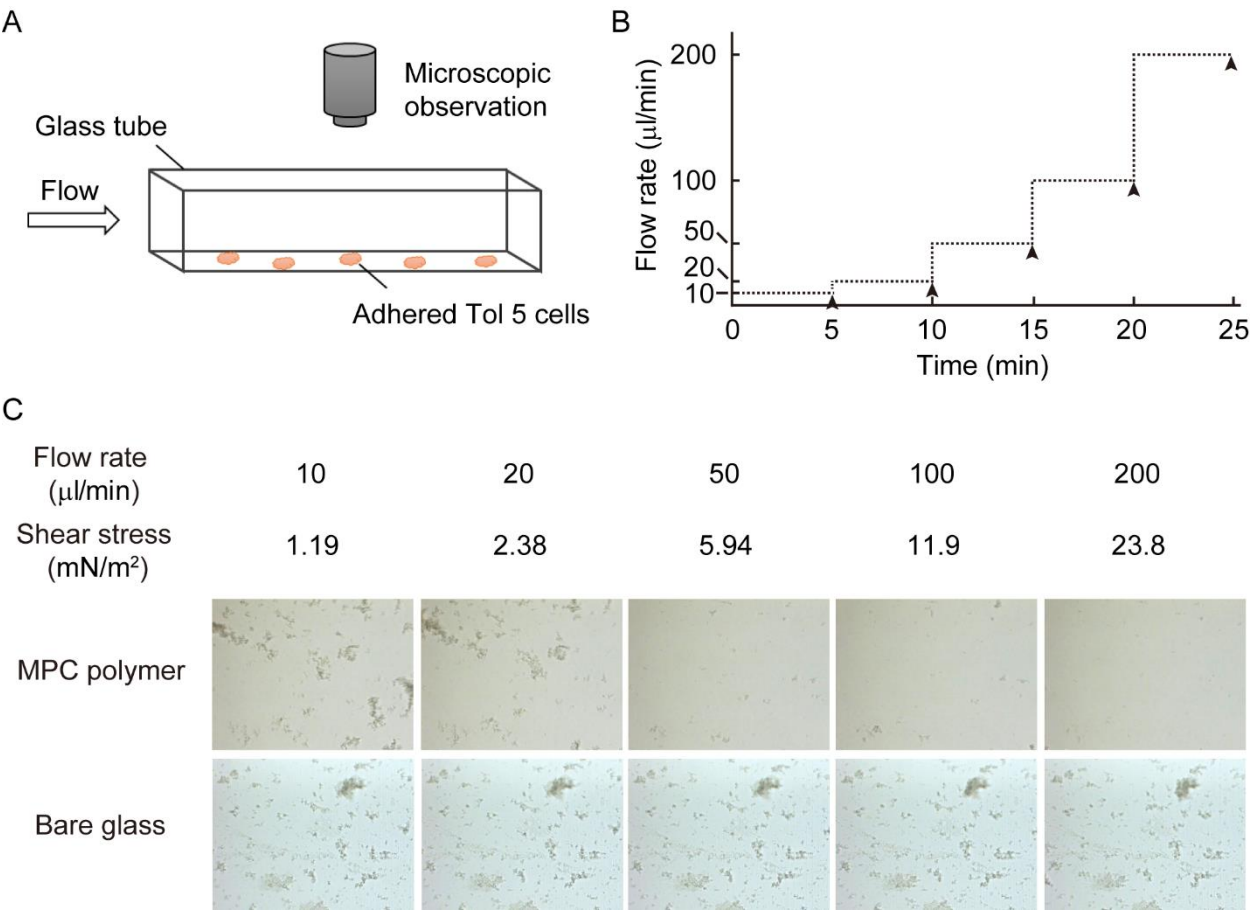


Fig. 4. Observation of the behavior of Tol 5 cells that were adhered to the MPC polymer surface beforehand. (A) Schematic representation of the flow cell system used in this study. (B) Transition of the flow rate. The flow rate was increased stepwise every 5 min. The black arrowheads indicate the time at which snapshots of the inner surface at the bottom of the glass tubes were captured. (C) The snapshots captured as described in (B).

Supplementary Materials

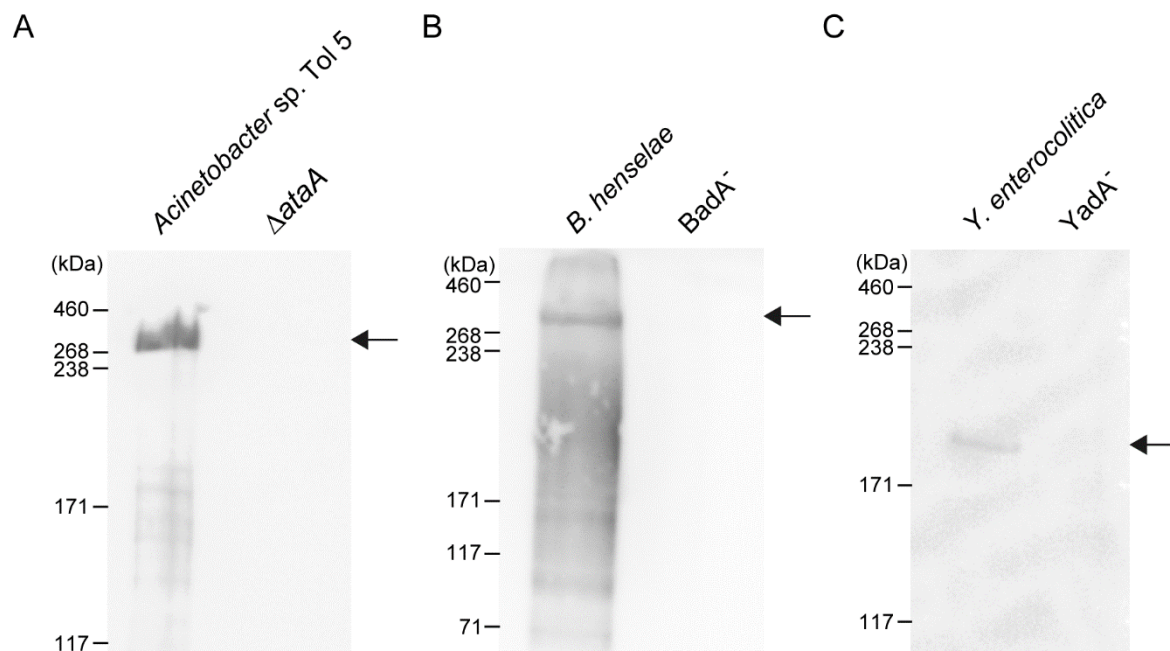


Fig. S1. Production of trimeric autotransporter adhesin (TAA) in each bacterial cell. Cell lysates of *Acinetobacter* sp. Tol 5 (A), *B. henselae* (B), and *Y. enterocolitica* (C) were separated by SDS-PAGE with their TAA-less mutant strains, and each TAA was detected by western blotting. The arrow in each panel indicates the band corresponding to AtaA monomer (A), BadA monomer (B), and YadA trimer (C).

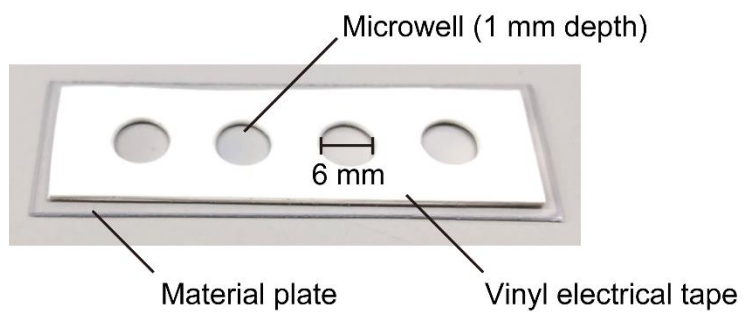


Fig. S2. Preparation of microwells on material surfaces. Four sheets of vinyl electrical tape were piled up and holes with a diameter of 6 mm were punched. The punched tapes were placed on a material plate.

386 **Table S1. Bacterial strains used in this study.**

Strain	Description	Reference
<i>Acinetobacter</i> sp. Tol 5	Wild type strain, expressing <i>ataA</i>	(14)
<i>Acinetobacter</i> sp. Tol 5 Δ <i>ataA</i>	<i>Acinetobacter</i> sp. Tol 5 4140, Unmarked Δ <i>ataA</i> mutant of Tol 5, <i>ataA</i> ⁻	(34)
<i>Bartonella henselae</i>	<i>B. henselae</i> Marseille, Patient isolate, expressing <i>badA</i>	(35)
<i>Bartonella henselae</i> BadA ⁻	<i>B. henselae</i> Marseille transposon mutant, transposon integrated in <i>badA</i> , Km ^r	(31)
<i>Yersinia enterocolitica</i>	<i>Y. enterocolitica</i> WA-314 serotype O:8, harboring plasmid pYV, expressing <i>yadA</i>	(36)
<i>Yersinia enterocolitica</i> YadA ⁻	<i>Y. enterocolitica</i> WA-C, plasmid less derivative of WA-314, <i>yadA</i> ⁻	(36)

387
388

389 **Table S2. Static contact angles (SCA) of air in water of material surfaces.**

390

Material	Polystyrene	Glass	Stainless steel	PTFE	Mica	Poly(mOEGMA) brush	MPC polymer
SCA [deg]	99 ± 2	139 ± 3	101 ± 3	86 ± 4	142 ± 3	134 ± 2	154 ± 4

391 Data are expressed as the mean ± SD (n = 5).

392

Movie S1. Detachment of adhered Tol 5 cells from the MPC polymer coated glass. A glass tube with or without an MPC polymer coating was filled with Tol 5 cell suspension and incubated for 10 min. Then, the cell suspension was replaced with fresh BS-N medium by slow flowing at 10 μ L/min for 35 min, and the flow rate was increased stepwise as shown in Figure 4B. Live images of the adhesion behavior of Tol 5 cells on the inner surface of the glass tubes were observed with a digital microscope.